[14]D. O. Van Ostenburg, H. D. Trapp, and D. J. Lam, Phys. Rev. 126, 938 (1962).
[15]D. O. Van Ostenburg, J. J. Spokas, and D. J. Lam, Phys. Rev. 139, 713 (1965).
[16]M. Bernasson, P. Descouts, P. Donzé, and A. Treyvaud, J. Phys. Chem. Solids 30, 2453 (1969).
[17]D. O. Van Ostenburg, D. J. Lam, H. D. Trapp, D. W. Pracht, and T. J. Rowland, Phys. Rev. 135, 455 (1964).
[18]A. J. Maeland, J. Phys. Chem, 68, 2197 (1964).
[19]E. von Meerwall and D. S. Schreiber, Phys. Letters 27, 574 (1968).
[20]L. E. Drain, *Proceedings of the XIII Colloque Ampère Amsterdam*, 1964 (North-Holland, Amsterdam, 1965), p. 181.
[21]E. von Meerwall and T. J. Rowland, Solid State Commun. 9, 305 (1971).
[22]G. Hörz, Z. Metallk. 61, 371 (1970); 60, 50 (1969).
[23]R. H. Geils, Rev. Sci. Instr. 42, 266 (1971).
[24]T. G. Berlincourt and R. R. Hake, Phys. Rev. 131, 140 (1963).
[25]For all work on transition-metal alloys in this study, the same specimen of Leico V has been used as intensity reference.
[26]B. T. Feld and W. E. Lamb, Jr., Phys. Rev. 67, 15 (1945); R. V. Pound, *ibid.* 79, 685 (1950).
[27]K. Kambe and J. F. Ollom, J. Phys. Soc. Japan 11, 50 (1956).
[28]W. B. Pearson, *A Handbook of Lattice Spacings and Structures of Metals and Alloys* (Pergamon, New York, 1958), Vol. I; *ibid.* (Pergamon, New York, 1967), Vol. II.
[29]W. Kohn and S. H. Vosko, Phys. Rev. 119, 912 (1960).
[30]R. E. Watson, A. C. Gossard, and Y. Yafet, Phys. Rev. 140, A375 (1965).
[31]R. M. Sternheimer, Phys. Rev. 96, 951 (1954).
[32]C. H. Cheng, C. T. Wei, and P. A. Beck, Phys. Rev. 120, 426 (1960).
[33]A. J. Freeman and R. E. Watson, in *Treatise of Magnetism*, edited by R. H. Suhl and G. T. Rado (Academic, New York, 1965), Vol. IIA.
[34]A. M. Clogston, A. C. Gossard, V. Jaccarino, and Y. Yafet, Phys. Rev. Letters 9, 262 (1962).

PHYSICAL REVIEW B VOLUME 5, NUMBER 7 1 APRIL 1972

New Technique for Determining the Diffusion Mechanism by NMR: Application to Cl^{35} Diffusion in TlCl†

Gary L. Samuelson* and David C. Ailion
Department of Physics, University of Utah, Salt Lake City, Utah 84112
(Received 16 August 1971)

A major problem in the study of atomic motions is the determination of the dominant mechanism responsible for translational diffusion. Recently Ailion and Ho predicted that the rotating-frame spin-lattice relaxation time $T_{1\rho}$ would have an angular dependence which depends on the diffusion mechanism in the ultraslow-motion region. In this paper we have extended these ideas to TlCl for which the dominant mechanism is known by other experiments to be Cl vacancy diffusion. We observed experimentally an angular dependence consistent with the dominant mechanism being Cl vacancy diffusion, thereby corroborating the basic ideas of Ailion and Ho. We have also been able to eliminate Cl interstitialcy diffusion as a possible dominant mechanism. We measured an activation energy of (0.733 ± 0.012) eV, in agreement with results of other experiments.

I. INTRODUCTION

In this paper we report the experimental verification of a new technique for determining diffusion mechanisms in solids.[1] This technique was proposed theoretically by Ailion and Ho,[2] who predicted that in the ultraslow-motion region[3] the rotating-frame spin-lattice relaxation time $T_{1\rho}$ would depend upon the angle which the external magnetic field H_0 makes with respect to the crystal axes. In particular they predicted that this angular dependence could vary significantly with diffusion mechanism and could, for example, be measurably different for vacancy, interstitialcy, and interstitial diffusion. Direct comparison of the experimental data with the results of calculations could then be used to distinguish the dominant mechanism from alternate possibilities.

We chose to perform our experimental study on a solid for which the diffusion mechanism has been determined to a high degree of probability by other techniques. In particular we studied TlCl for which the dominant mechanism, as determined by Friauf,[4] is chlorine vacancy diffusion. Our results are in excellent agreement with the results of Friauf and strongly corroborate the ideas of Ailion and Ho.

II. BACKGROUND

A. Strong-Collision Theory

The theoretical calculations for $T_{1\rho}$ in TlCl utilize the strong-collision approach, originally developed by Slichter and Ailion[5] (SA). We now review the strong-collision theory and the conditions under which it is valid. The motivation for a strong-collision theory arises when we attempt to study the spin-lattice relaxation time in very weak Zeeman fields. Under conditions such that the external magnetic field is less than or comparable to the local field, weak-collision[6–8] theories which

treat the fluctuating dipolar Hamiltonian as a perturbation on the Zeeman system break down and must be replaced with a nonperturbation (strong-collision) theory.

The strong-collision theory was originally developed in order to relate the experimentally measured spin-lattice relaxation time in the ultra-slow-motion region to the atomic-diffusion correlation time τ. According to Bloembergen, Purcell, and Pound (BPP),[6] atomic diffusion will result in a maximum in the spin-lattice relaxation rate (i.e., a T_1 minimum) when $\tau \sim 1/\omega_0$, where ω_0 is the Larmor frequency. If we perform our experiment in weak applied field, the T_1 minimum will correspond to a longer value of τ occurring at lower temperatures. (In zero field, SA[9] showed that the T_1 minimum would occur at the onset of motional narrowing; i.e., at $\tau \approx T_2$.) We thus see that an ability to study spin-lattice relaxation in weak fields is essential to the observation of "ultra-slow motions" (i.e., motions for which $\tau \gg T_2$ which occur in the rigid lattice at temperatures below the onset of motional narrowing).

A commonly used method for studying weak-field relaxation is to demagnetize the field adiabatically and then to remagnetize adiabatically. By waiting a variable time in the demagnetized state and then plotting the signal in the remagnetized state, we can determine the weak-field relaxation time.[10] In order to satisfy easily the somewhat conflicting requirements that the demagnetization occur sufficiently slowly to satisfy the adiabatic condition[11] and yet occur in a time short compared to the relaxation time, it is usually convenient to perform the demagnetization in the rotating frame.[9,12,13]

The theory of SA is based on two assumptions. The first is that sufficient time elapses between diffusion jumps for the dipolar and Zeeman systems to come to thermal equilibrium between jumps. This assumption allows us to assign a temperature to the spin system prior to each jump. We can then assign to the spin system a density operator[14]

$$\rho = e^{-\mathcal{H}/k\theta}/Z \ . \tag{1}$$

(If we perform our experiment in the rotating frame, we must replace $\mathcal{H}$ by $\mathcal{H}^0$, the rotating-frame Hamiltonian.[12]) The use of this equilibrium density matrix enables us to calculate the expectation values of quantities like the magnetization and energy without first determining the wave functions, since expectation values can be expressed as traces which are independent of representation:

$$\langle \vec{M} \rangle = \mathrm{Tr}(\rho \vec{M}) \tag{2a}$$

and

$$\langle \mathcal{H}^0 \rangle = \mathrm{Tr}(\rho \mathcal{H}^0) \ . \tag{2b}$$

Since the time required for the dipolar and Zeeman systems to come to thermal equlibrium is given by the cross-relaxation time T_{cr} (which is approximately equal to T_2 for fields comparable to or less than the local field), and since the mean time an atom sits between jumps is the correlation time τ, this assumption will be valid provided $\tau \gg T_2$. Thus, the strong-collision theory will complement the weak-collision theories in that the former applies in the rigid-lattice region on the low-temperature side of the weak-field T_1 minimum, whereas the latter applies to the motionally narrow region above the minimum.

The second assumption of the strong-collision theory is that the same equilibrium density matrix can be used to calculate the spin energy immediately before and immediately after the atomic jump. This assumption is equivalent to the sudden approximation in that the effect of diffusion is to cause, from the point of view of the jumping nucleus, a sudden change in the dipolar Hamiltonian but not in the density matrix. In other words we are assuming that the time the nucleus spends in the actual process of jumping is sufficiently short that, immediately after a diffusion jump, the spin will have the same orientation as it had immediately before the jump. If this assumption were not satisfied because the nucleus jumped so slowly that it had time to align itself along the new local field, the jumping would not result in a change in dipolar order and would not be observable by magnetic resonance. Using the sudden approximation we can calculate the energy change resulting from a jump:

$$\langle \Delta E \rangle = \langle \mathcal{H}_f^0 \rangle - \langle \mathcal{H}_i^0 \rangle = \mathrm{Tr}[\rho(\mathcal{H}_f^0 - \mathcal{H}_i^0)] \ , \tag{3}$$

where $\mathcal{H}_i^0$ and $\mathcal{H}_f^0$ are the initial and final values of the spin Hamiltonian, respectively.

B. Calculation of $(T_{1\rho})_{diff}$

The considerations leading to an expression for $(T_{1\rho})_{diff}$, the diffusion contribution to $T_{1\rho}$, have been described in detail elsewhere.[2,3,5,15] Accordingly, we shall outline them only briefly here.

The original treatment of SA applied to the case where only dipolar interactions contribute to the energy change resulting from a jump. More recently, Rowland and Fradin[15] (RF) and Wagner and Moran[16] extended their treatment to the case where quadrupolar interactions are also present.

For a rotating-frame Hamiltonian consisting of Zeeman, dipolar, and quadrupolar terms, we obtain

$$\mathcal{H}^0 = \mathcal{H}_Z^0 + \mathcal{H}_D^0 + \mathcal{H}_Q^0 \ . \tag{4}$$

Using the high-temperature approximation, the total average spin energy can be calculated and written in the form

$$\langle \mathcal{H}^0 \rangle = -\frac{C_I(H_D^2 + H_Q^2 + H_{eff}^2)}{\theta} \ . \tag{5}$$

H_D is the dipolar contribution to the local field and H_Q is the equivalent local field arising from the quadrupolar interactions. $\vec{H}_{eff}$ is the rotating-frame Zeeman field and equals $H_1\vec{i} + (H_0 - \omega/\gamma)\vec{k}$; C_I is the Curie constant for I spins $N_I \gamma_I \hbar I(I+1)/3k_B$; and θ is the prejump equilibrium temperature. Since $\langle \Delta E \rangle$ is also proportional to $1/\theta$, the fractional energy change $\langle \Delta E \rangle / \langle \mathcal{H}^0 \rangle$ is independent of the equilibrium temperature. From this consideration, we can now relate $(T_{1\rho})_{diff}$ to the jump correlation time τ. We let N_I be the total number of I spins each of which jumps on the average once in a time τ. We can write the rate of energy change as

$$\frac{\partial \langle \mathcal{H}^0 \rangle}{\partial t} = \frac{\partial \langle \mathcal{H}_D^0 \rangle}{\partial t} + \frac{\partial \langle \mathcal{H}_Q^0 \rangle}{\partial t} + \frac{\partial \langle \mathcal{H}_Z^0 \rangle}{\partial t}$$

$$= \frac{N_I}{\tau}\left(\frac{\langle \Delta E \rangle_D}{\langle \mathcal{H}_D^0 \rangle} \langle \mathcal{H}_D^0 \rangle + \frac{\langle \Delta E \rangle_Q}{\langle \mathcal{H}_Q^0 \rangle} \langle \mathcal{H}_Q^0 \rangle \right) + \frac{\partial \langle \mathcal{H}_Z^0 \rangle}{\partial t} . \quad (6)$$

SA defined the dipolar-order parameter p_D by letting $NI\langle \Delta E \rangle_D / \langle \mathcal{H}_D^0 \rangle$ equal $-2(1-p_D)$ and RF used[15] a similar definition for the quadrupolar-order parameter: $N_I \langle \Delta E \rangle_Q / \langle \mathcal{H}_Q^0 \rangle = -(1-p_Q)$. We can thus think of p_D and p_Q as parameters which describe, respectively, the loss of dipolar and quadrupolar order resulting from a jump. It is easy to show[3] that these considerations lead to the following relaxation equation for the magnetization $\langle M \rangle$ in the rotating frame:

$$\frac{\partial \langle M \rangle}{\partial t} = \frac{(M_{eq} - \langle M \rangle)}{T_{1\rho}} , \quad (7)$$

where M_{eq} is the thermal equilibrium magnetization. The diffusion contribution $(T_{1\rho})_{diff}$ can be shown[3] to be given by

$$(T_{1\rho})_{diff} = \frac{\tau(H_1^2 + H_D^2 + H_Q^2)}{2(1-p_D)H_D^2 + (1-p_Q)H_Q^2} . \quad (8)$$

This formula reduces to the SA result[5] when $H_Q = 0$.

III. THEORY

A. Calculation of H_D^2

In this section, we calculate the quantities H_D^2 and $(1-p_D)$ in order to derive a theoretical expression for $(T_{1\rho})_{diff}$ in TlCl for chlorine diffusion. Toward the end of this section we discuss τ, H_Q^2, and $(1-p_Q)H_Q^2$ which have been experimentally determined.

Before going from Eq. (2b) to Eq. (8), we first define the dipolar local field H_D as follows:

$$H_D^2 \equiv \frac{\mathrm{Tr}(\mathcal{H}_D^0)^2}{C_I k Z} , \quad (9)$$

where Z is the partition function. Using Eq. (2b), we then see that

TABLE I. TlCl data.[a]

Isotope	% abundance	$\gamma/2\pi$ MHz/10^4 G	Spin	Quadrupole moment
Cl^{35}	75.4	4.172	$\frac{3}{2}$	-0.079×10^{-24} cm^2
Cl^{37}	24.6	3.472	$\frac{3}{2}$	-0.062×10^{-24} cm^2
Tl^{203}	29.52	24.33	$\frac{1}{2}$	0
Tl^{205}	70.48	24.57	$\frac{1}{2}$	0

[a]These data were obtained from the Varian NMR Table (fourth edition).

$$\langle \mathcal{H}_D^0 \rangle = -\frac{\mathrm{Tr}(\mathcal{H}_D^0)^2}{k\theta Z} = -\frac{C_I H_D^2}{\theta} . \quad (10)$$

From this relation and the previous definition for $(1-p_D)$, we obtain

$$(1-p_D) = \frac{N_I \theta \langle \Delta E \rangle_D}{2C_I H_D^2} . \quad (11)$$

Table I lists isotopic data on TlCl which show that both chlorine and thallium consist of two abundant isotopes. We thus have a four-spin system with two-spin species on each sublattice. The dipolar Hamiltonian $\mathcal{H}_D^0$ can then be broken down into ten interactions. In order to describe these interactions, the following definitions are made: Spin numbers I and I' will refer to the Cl^{35} and Cl^{37} isotopes, respectively, and S and S' to the Tl^{205} and Tl^{203} isotopes, respectively. Indices i and j refer to chlorine spins and s and t to the thallium spins. If N represents the total number of chlorine spins in our sample, we can define the fractions $f_I = N_I/N$, $f_{I'} = N_{I'}/N$, $f_S = N_S/N$, and $f_{S'} = N_{S'}/N$, where $N_I + N_{I'} = N_S + N_{S'} = N$. There are several different types of terms in the rotating-frame dipolar Hamiltonian. The like-like contribution is

$$\mathcal{H}_{DII} = \frac{\gamma_I^2 \hbar^2}{2a^3} \frac{1}{2} \sum_{i,j} C_{ij}(I_{iz}I_{jz} - 3\vec{I}_i \cdot \vec{I}_j) , \quad (12)$$

where

$$C_{ij} \equiv \frac{(1 - 3\cos^2\theta_{ij})}{r_{ij}^3} , \quad (13)$$

and where θ_{ij} is the angle between the internuclear vector $\vec{r}_{ij}$ and $\vec{H}_0$. The lattice parameter a has been factored out so that the internuclear distance r_{ij} is in units of a.

Equation (12) is a like-like spin interaction on the same sublattice. We also have two interaction terms, $\mathcal{H}_{DII'}^0$, and $\mathcal{H}_{DSS'}^0$, which involve interactions between unlike spins on the same sublattice, and have the form

$$\mathcal{H}_{DII'}^0 = \frac{\gamma_I \gamma_{I'} \hbar^2}{a^3} \sum_{i,j} C_{ij} I_{iz} I'_{jz} . \quad (14)$$

Finally we have a term describing interactions between unlike spins on different sublattices:

$$\mathcal{H}^0_{DIS} = \frac{\gamma_I \gamma_S \hbar^2}{a^3} \sum_{i,s} C_{is} I_{iz} S_{sz} \,. \tag{15}$$

Using Eq. (11) we can obtain the ten contributions to $\langle \mathcal{H}^0_D \rangle$ by performing standard trace calculations involving squares of the terms in the Hamiltonian. From $\mathcal{H}^0_{DII}$, we obtain

$$\langle \mathcal{H}^0_{DII} \rangle = -\frac{\hbar^4 \gamma_I{}^4 I^2 (I+1)^2}{12 k \theta a^6} N_I f_I \sum_i C_{ij}{}^2 \,. \tag{16}$$

In the above we have replaced the sum over j by a factor N_I representing the number of equivalent Cl^{35} sites. We introduce the factor f_I in order for the index i to range over all N lattice sites rather than those belonging to I spins. We assume that the I spins are randomly distributed over the chlorine sublattice. Using similar arguments,[17] we obtain

$$\langle \mathcal{H}^0_{DII'} \rangle = -\frac{\hbar^4 \gamma_I{}^2 \gamma_{I'}{}^2 I(I+1) I'(I'+1)}{9 k \theta a^6} N_I f_{I'} \sum_i C_{ij}{}^2 \tag{17}$$

and

$$\langle \mathcal{H}^0_{DIS} \rangle = -\frac{\hbar^4 \gamma_I{}^2 \gamma_S{}^2 I(I+1) S(S+1)}{9 k \theta a^6} N_I f_S \sum_s C_{sj}{}^2 \,. \tag{18}$$

Combining all ten contributions and grouping terms, we have

$$H_D{}^2 = -\frac{\theta}{C_I} \langle \mathcal{H}^0_D \rangle = \frac{\hbar^2 f_I \gamma_I{}^2 I(I+1)}{4a^6} \left\{ \left[1 + \frac{4 f_{I'} \gamma_{I'}{}^2}{3 f_I \gamma_I{}^2} + \frac{f_{I'}{}^2 \gamma_{I'}{}^4}{f_I{}^2 \gamma_I{}^4} + \frac{f_S{}^2 \gamma_S{}^4 S^2 (S+1)^2}{f_I{}^2 \gamma_I{}^4 I^2 (I+1)^2} \left(1 + \frac{4 f_{S'} \gamma_{S'}{}^2}{3 f_S \gamma_S{}^2} + \frac{f_{S'}{}^2 \gamma_{S'}{}^4}{f_S{}^2 \gamma_S{}^4} \right) \right] \sum_i C_{ij}{}^2 \right.$$
$$\left. + \frac{4 f_S \gamma_S{}^2 S(S+1)}{3 f_I \gamma_I{}^2 I(I+1)} \left(1 + \frac{f_{I'} \gamma_{I'}{}^2}{f_I \gamma_I{}^2} \right) \left(1 + \frac{f_{S'} \gamma_{S'}{}^2}{f_S \gamma_S{}^2} \right) \sum_s C_{sj}{}^2 \right\} . \tag{19}$$

In order to perform the lattice sums $\sum_i C_{ij}{}^2$ and $\sum_s C_{sj}{}^2$, we employed a procedure similar to that used in the Appendix of the paper by Ailion and Ho.[2] The other data needed to evaluate Eq. (19) appear in Table I. If we take the lattice parameter a to be 3.846×10^{-8} cm, we obtain for $H_D{}^2$,

$$H_D{}^2 = (1.666 - 0.548 \sin^2 2\varphi)\, G^2 \,, \tag{20}$$

where the angle φ is measured between the crystal $\langle 100 \rangle$ axis and the static field $\vec{H}_0$.

B. Calculation of $(1 - p_D)$

In the calculation of $(1 - p_D)$, we must derive expressions for the initial and final Hamiltonians which describe the specific jump mechanism under study. Then, by using Eqs. (3), (11), and (20), we can obtain the value of $(1 - p_D)$ related to that particular jump mechanism.[18]

As we observed in Sec. II, an essential requirement of the theory of SA is that the atoms jump sufficiently infrequently that $\tau \gg T_2$ in order for the spin-temperature assumption to be satisfied prior to each jump. Since typically diffusion results from the motion of a *small* concentration of defects (such as vacancies or interstitials), we must consider two special cases. First we observe that the mean time τ_d that a defect spends between jumps is related to the mean time τ that an atom spends between its jumps by means of the following relation:

$$\tau_d = (N_d / N)\, \tau \,, \tag{21}$$

where N_d/N represents the defect (e.g., vacancy or interstitial) concentration. We thus have the possibility that $\tau_d \ll T_2$ even though $\tau \gg T_2$. This means that the defect produces along its path a trail of neighboring spins which individually have not approached semiequilibrium and are thus "hot." Since the time between encounters[19] is of order τ, the effect of the encounter is to cause a displacement of the spins in the trail. By calculating the energy change of the entire hot-spin trail and then dividing by the number of spins involved, we can obtain the average energy change per jumping spin.[20] The second case occurs when $\tau_d \gg T_2$ (this is the case originally considered by SA). In this case every spin on the defect's path will attain equilibrium prior to the next jump of the defect. For typical low defect concentrations this second condition can be achieved only at low temperatures. Under typical experimental conditions, τ_d will be less than T_2. Therefore we shall now calculate $1 - p_D$ for the case $\tau_d \ll T_2 \ll \tau$ for vacancy diffusion in TlCl. (We shall calculate the results for the case $\tau_d \gg T_2$ in the Appendix).

In calculating the energy change $\langle \Delta E \rangle_D$ resulting from the jumping of an I spin (i.e., Cl^{35}), we must consider four kinds of terms: $\langle \Delta E_{II} \rangle_D$, $\langle \Delta E_{II'} \rangle_D$, $\langle \Delta E_{IS} \rangle_D$, and $\langle \Delta E_{IS'} \rangle_D$. Evaluating Eq. (3) for the dipolar contribution to $\langle \Delta E \rangle_D$ for the II interaction, we obtain

$$\langle \Delta E_{II} \rangle_D = \frac{\hbar^4 \gamma_I{}^4 I^2 (I+1)^2}{6 k \theta a^6} \frac{1}{2} \left(\sum_{i,j} C_{ij}{}^2 - \sum_{i,j} C_{ij} (C_{ij})' \right) . \tag{22}$$

The factor $(C_{ij})'$ comes from $\mathcal{H}^0_{DIIf}$ and is the value of C_{ij} immediately after an encounter. We can define g and h to be a subset of the indices i and j, respectively, which refers only to the jumping spins along the path of the vacancy. Since only the terms

for which either i or j corresponds to g or h can change as a result of a particular encounter, we can write these terms explicitly and cancel the rest. If we do so and combine equivalent terms involving i and j (which refer to the same terms), we obtain

$$\langle \Delta E_{II} \rangle_D = \frac{\hbar^4 \gamma_I^4 I^2 (I+1)^2}{6k\theta a^6} \left[\sum_{\substack{i \neq g \\ h}} C_{ih}^2 + \tfrac{1}{2} \sum_{g,h} C_{gh}^2 - \sum_{\substack{i \neq g \\ h}} C_{ih}(C_{ih})' - \tfrac{1}{2} \sum_{g,h} C_{gh}(C_{gh})' \right]. \quad (23)$$

If we assume the vacancy motion to be random, then any h spin can be treated as a typical spin. Then each of the h spins will on the average contribute equally to the sum. We can thus replace our sum over h by a factor n representing the number of spins in the trail. We will replace the running index h by a fixed index r which refers to a particular spin of interest; the g coordinates will then refer to other atoms *on the trail*. We can now replace the quantity in square brackets in Eq. (23) by

$$n \left[\sum_{i \neq g} C_{ir}^2 + \tfrac{1}{2} \sum_{g} C_{gr}^2 - \sum_{i \neq g} C_{ir}(C_{ir})' - \tfrac{1}{2} \sum_{g} G_{gr}(C_{gr})' \right]. \quad (24)$$

We shall now replace the spin sum with a lattice sum letting i range over all N sublattice sites. In order to account for the I' isotopes, we shall multiply the sum over lattice sites by f_I, the fraction of the spins which are I spins. The restriction $i \neq g$ can be removed by subtracting explicitly from the sum over all sites the terms for which $i = g$.

If we wish to consider only jumps which contribute to the dipolar relaxation, we must account for the possibility that one out of six jumps in the TlCl lattice will return a spin to its previous site. For $\tau_d \ll T_2$, this second jump effectively cancels the relaxation contribution of the previous jump. In general, if there are G nearest neighbors to a vacancy, then the contributing jumps are reduced by the factor $(G-2)/G$. Out of the five remaining jump directions which do contribute (ignoring the less likely possibility that a higher-order path may return the spin to its original site[18]) there is a $\frac{1}{5}$ probability that the vacancy will continue in the forward direction and a $\frac{4}{5}$ probability that it will move at right angles relative to the previous jump. If r is the initial site of the jumping atom of interest and q is its final site, we can designate nearest-neighbor sites to r in the following way. The site in line with r and q is labeled l and the four equivalent sites at right angles to the line of r and q are labeled t. Corresponding sites located about q will be m and n, respectively (see Fig. 1). The vacancy movement will result in the atom originally at sites l or t being transferred to site r, the atom at r moving to site q, and the atom at q going to sites n or m. A reasonable approximation is to consider the summation over g as including only terms arising from atoms in a region around r and q which contains only sites t, l, m, or n. Since the C_{ij}'s are proportional to r_{ij}^{-3}, we can neglect contributions from atoms on the "hot"-spin trail which are not nearest neighbors to r or q. We shall average over the four equivalent t and n sites.

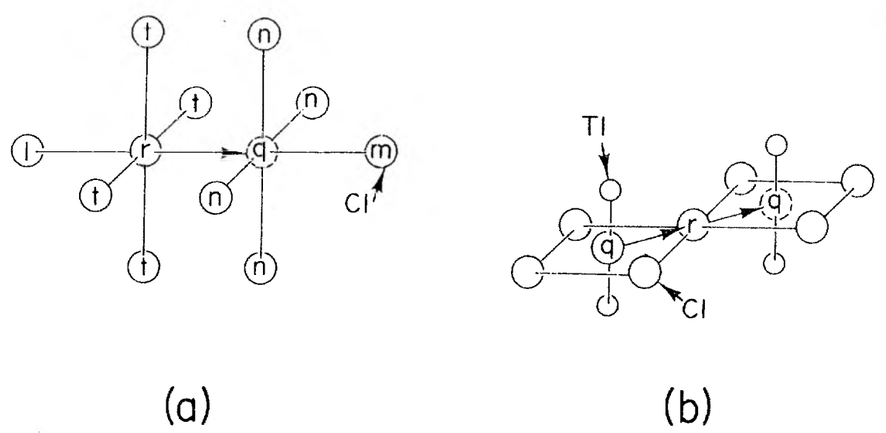

FIG. 1. Jump models describing diffusion in thallium chloride: (a) vacancy diffusion and (b) interstitialcy diffusion.

The II' interaction will have the same lattice sums as the II interaction since the I' spins occupy the same sublattice as the I spins. The difference is that the coefficient before the sum contains $\gamma_{I'}$ and $f_{I'}$ as well as a slightly different numerical factor. The energy change per spin on the chlorine sublattice is then obtained by dividing by the factor n.

The IS and IS' interactions will not involve the vacancy trail since the thallium atoms are fixed in position. The isotope concentrations are accounted for as before with the factors f_S and $f_{S'}$ when going from a spin to a lattice sum. Evaluating $(1-p_D)$ for the case $\tau_d \ll T_2$ from Eqs. (3), (11), and (20), we obtain

$$(1-p_D) = \frac{\hbar^2 f_I \gamma_I^2 I(I+1)}{4a^6 H_D^2} \left[\left(1 + \frac{2 f_{I'} \gamma_{I'}^2}{3 f_I \gamma_I^2} \right) \left(\sum_i C_{ir}^2 - C_{qr}^2 - \sum_i C_{ir} C_{iq} - \tfrac{1}{2} (\tfrac{1}{5} C_{mr}^2 + \tfrac{4}{5} C_{nr}^2) + 2(\tfrac{1}{5} C_{lr} C_{lq} + \tfrac{4}{5} C_{tr} C_{tq}) \right.\right.$$
$$\left.\left. - (\tfrac{1}{5} C_{lr} C_{rq} + \tfrac{4}{5} C_{tr} C_{rq}) \right) + \frac{2S(S+1)}{3I(I+1)} \left(\frac{f_S \gamma_S^2}{f_I \gamma_I^2} + \frac{f_{S'} \gamma_{S'}^2}{f_I \gamma_I^2} \right) \left(\sum_s C_{sr}^2 - \sum_s C_{sr} C_{sq} \right) \right]. \quad (25)$$

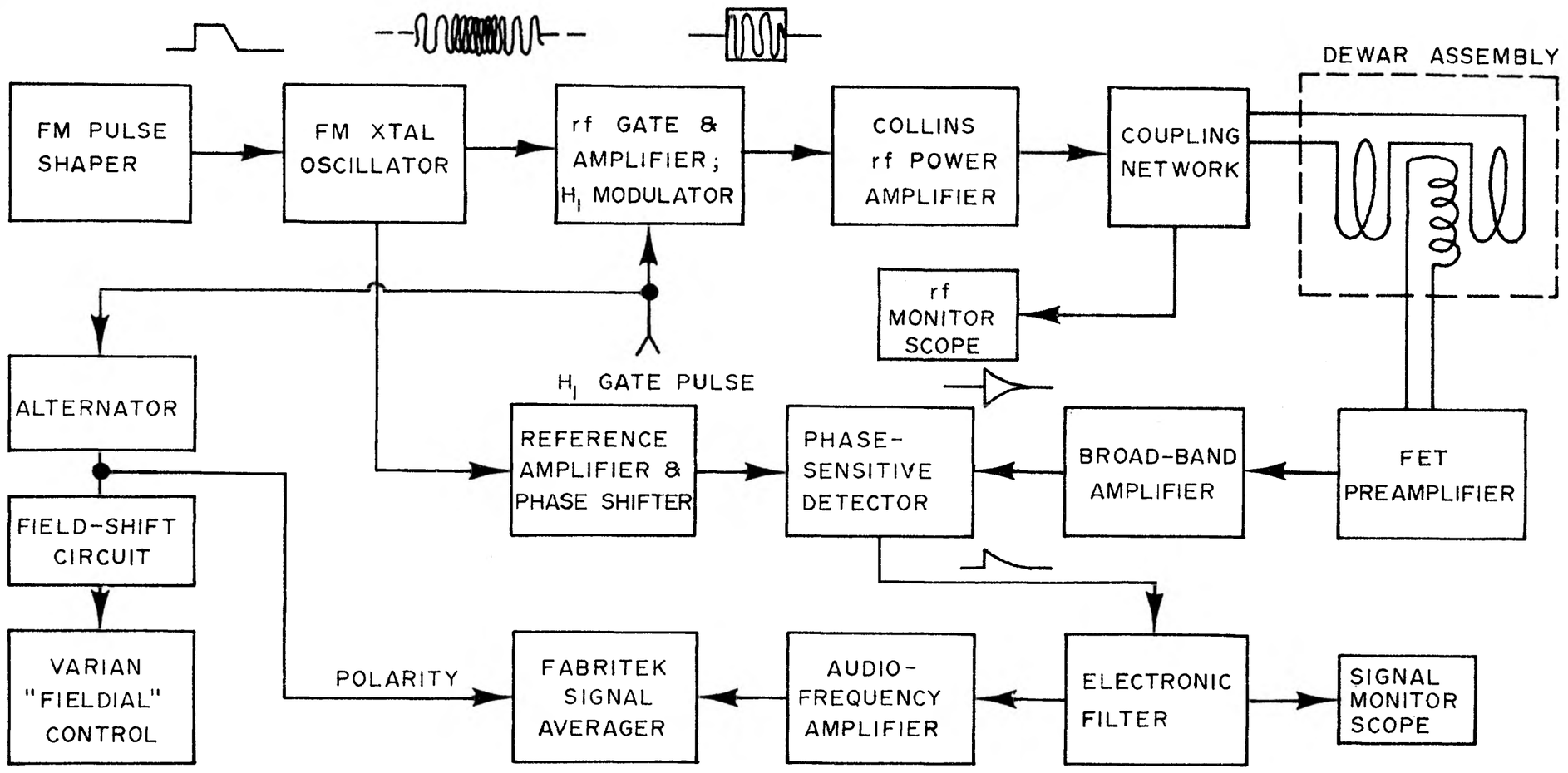

FIG. 2. Block diagram of pulse NMR apparatus.

If we evaluate all lattice sums for TlCl and use the parameters in Table I, we find the value of $(1-p_D)$ in Eq. (25) to be

$$(1-p_D)=\frac{0.0255+0.1936\sin^2 2\varphi}{1.666-0.548\sin^2 2\varphi}\,. \tag{26}$$

IV. APPARATUS

The apparatus[21] used in gathering data on the angular dependence of $(T_{1\rho})_{diff}$ is a cross-coil NMR spectrometer which provides a pulsed H_1 field of up to 7 G at a frequency of 4 MHz over a 12-cm^3 TlCl sample. Figure 2 comprises a block diagram of the basic components utilized in the system. In order to measure $T_{1\rho}$ it is necessary first to orient the magnetization parallel to H_1 in the rotating frame in the "spin-locked" configuration.[22] This process causes the temperature of the spin system to be reduced to a value lower than the lattice temperature. Under these conditions jumping results in a decrease in the magnetization as the spin temperature rises towards the lattice temperature. $T_{1\rho}$ is then measured by plotting the magnetization as a function of time in the spin-locked state. The magnetization, as measured by the amplitude of the free-induction decay following the turn-off of the rf pulse, will decrease with a time constant $T_{1\rho}$.

A. Description of Block Diagram

It is clear that, in order to measure $T_{1\rho}$, one must have a transmitter which can spin lock the magnetization and can also provide rf pulses which are long compared to $T_{1\rho}$ (which may be several seconds). In our system spin locking is achieved by means of adiabatic demagnetization in the rotating frame (ADRF). However, in contrast to the methods[9,13] which pulse the static field H_0, we demagnetize the rotating-frame effective field by modulating the rf frequency.[23] In order to obtain large shifts in H_{eff} by frequency modulation, 16- and 20-MHz crystal oscillators are "pulled" off frequency in opposite directions using voltage-controlled capacitative loading. The basic 4-MHz $\vec{H}_1$ frequency is then obtained by rf mixing. The modulating voltage is an upward step followed by a downward ramp. This ramp allows the system to be returned to exact resonance adiabatically so that the magnetization will then be spin locked along $\vec{H}_1$.

The cw output of the FM XTAL OSCILLATOR circuit is fed to a gating circuit similar to the one developed by Blume,[24] and then to a modified Heathkit 90-W amplifier. The Heathkit has been extensively modified[17] to provide the capability of demagnetizing $\vec{H}_1$ to zero (or to any level between zero and maximum) and of remagnetization back to the maximum. This second demagnetization provides a complete transfer of Zeeman order to the dipolar system. The rf output is further amplified by a Collins 30-S 1-kW linear amplifier before being applied to the sample's transmitter coil.

A convenient method has been devised for matching the transmitter coil (a cylindrical Helmholtz pair[25]) to the Collins output. The tuning and matching procedures have been "orthogonalized"[17] by series tuning and parallel matching with a π-coupling network. The coil's Q is controlled with an external noninductive series resistance which is placed outside the Dewar. By then using a coil of

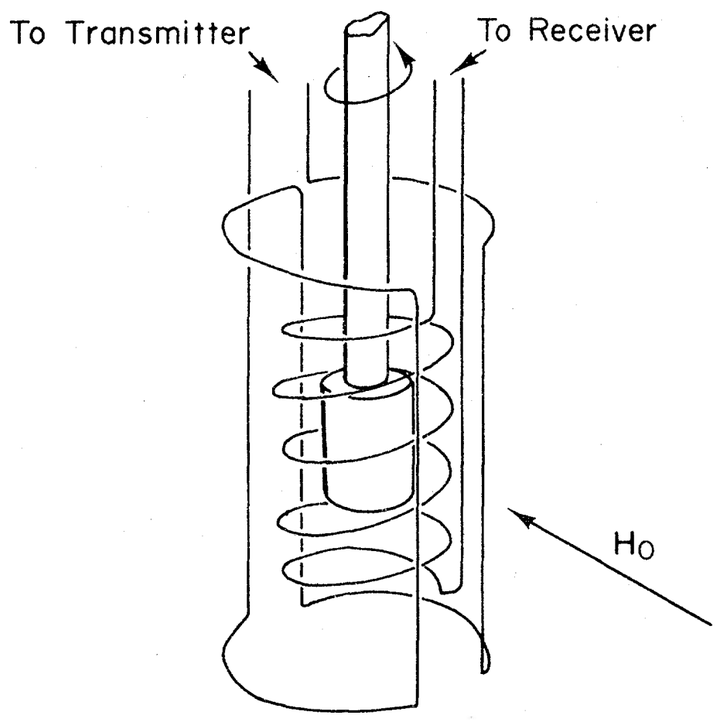

FIG. 3. Relation of transmitter and receiver coils to sample. The sample is mounted in a rotatable holder for angular studies.

fairly high Q, most of the heat energy is expended in the series resistance outside the Dewar thereby permitting more uniform temperature control. A self-switching solid-state damping circuit[26] has been installed in the matching network to reduce the transmitter ringdown time and to attenuate shot noise between pulses.

We see from Fig. 3 the arrangement of the transmitter and receiver coils. Ceramic forms are used for support and spacing. The receiver-coil assembly with sample can be removed by using a long stainless-steel tube extending down into the cryostat. An inner concentric tube is used to cross the receiver coil for minimum coupling with the transmitter, whereas a third is used to rotate the sample holder in order to do the angular studies. A calibrated dial attached to the inner tube is used to record the crystal orientation.

The preamplifier for the receiver consists mainly of a dual-gate FET cascode circuit.[17] Provision is made to clamp the input to ground for a few μsec after the $\vec{H}_1$ pulse in order to damp the receiver, thereby improving the recovery. This becomes essential in light of another feature of the preamplifier; by using positive feedback we are able to multiply the effective value of the receiver Q to several hundred for improved signal to noise. In order to observe the free-induction-decay shape, the Q is reduced for several μsec following the rf pulse turnoff thereby improving the receiver recovery. The magnetization signal is amplified by a wide-band amplifier and is then phase-sensitive detected. High-frequency noise is attenuated by passing the signal through an active low-pass filter. In order to improve further total system recovery we installed series FET gates before the broad-band amplifier and the low-pass filter for the purpose of blocking the $\vec{H}_1$ pulse.

The filtered-signal data are then processed by a Fabri-Tek 1074 multichannel averager.[27] The Fabri-Tek has been modified to subtract automatically the off-resonant signal from the resonant signal in an alternate manner so that only real resonance data is accumulated for multiple averaging. By this means we were able to eliminate nonresonant noise sources and offsets. This feature has been extremely useful in attenuating the effect of a noise source thought to be an electromechanical acoustic oscillation in the brass supports and shield near the transmitter coil.

Our Varian 12-in. magnet Fieldial control has been modified to alternate the field between two levels separated by an adjustable amount, typically about 100 G. The repeat time is adjusted to be longer than the settling-time response of the magnet controller to this step impulse. One of the levels is the on-resonance level, and it is synchronized with the Fabri-Tek polarity control so that a signal obtained during this time will be added to the accumulated data. The alternate magnetic field level is off resonance and is synchronized with the subtract mode of the Fabri-Tek so that everything but the resonance signal is removed from the memory.

B. Temperature-Control System

The cryostat has been designed to allow continuous control of temperatures from 90 to better than 400 °K by connecting to the sample head a cold tank and heater arrangement. The heater is placed close to the sample and is wound on the neck of the rf head. The heat leak to the cold tank can be adjusted by changing the number and composition of connecting rods connecting the sample head to the cold tank. The rods were composed of either copper or stainless steel depending on whether a strong or weak thermal coupling was desired. In order to achieve better thermal stability, the entire cryostat was mounted inside a Dewar.

The sample temperature was monitored with a calibrated platinum-resistance thermometer placed in direct contact with the sample. In order to improve the temperature stability, we employed a Leeds-and-Northrup proportional controller in a feedback loop between the heater and the thermometer. We were then easily able to hold the temperature variations to within ± 0.2 °K at each temperature.

V. EXPERIMENTAL RESULTS

We shall now describe the results of a number of experiments which we performed on TlCl.

In the $T_{1\rho}$ measurements, our technique is similar to that employed by SA except that, after adiabatically demagnetizing H_0, we performed an adia-

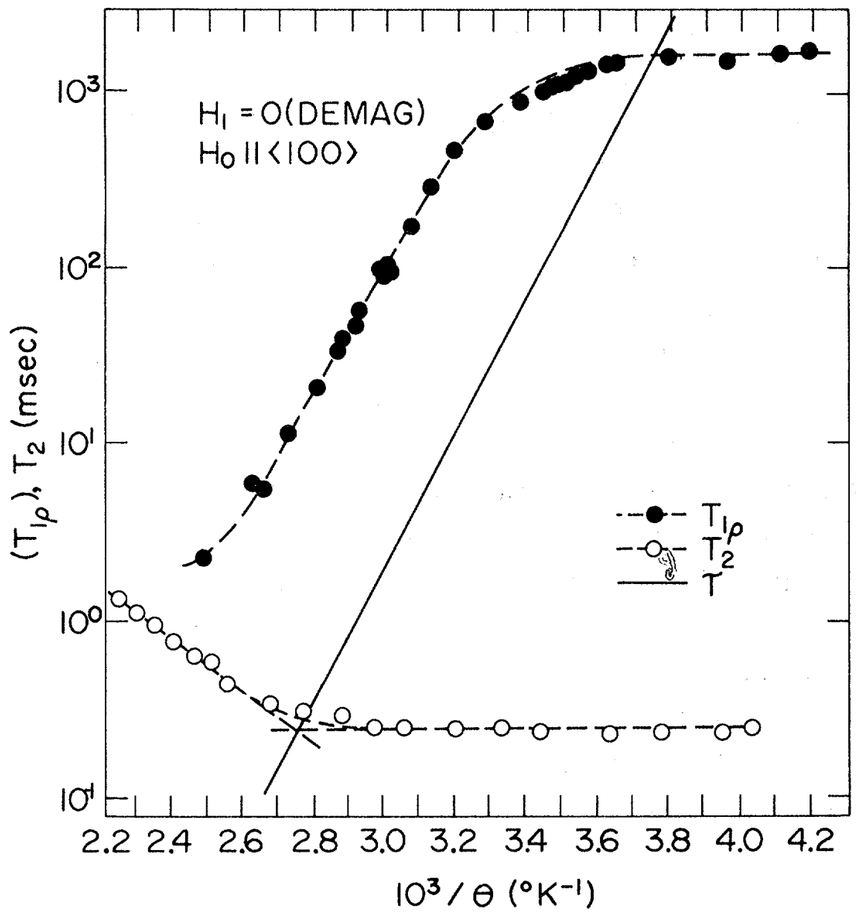

FIG. 4. $T_{1\rho}$ vs reciprocal temperature. T_2 vs reciprocal temperature is also plotted and illustrates the technique used to determine the value of τ at the temperature corresponding to the onset of motional narrowing. The T_2 data were taken in a powder.

batic demagnetization of H_1. Our pulse sequence is as follows. At $t=0$, we set H_0 exactly to resonance with $H_1=0$. We then turned on our H_1 at a frequency different from the resonant value and then performed an adiabatic demagnetization[28] in the rotating frame by letting the rf frequency (rather than the external field) slowly return to the resonant value.[23] Our off-resonance frequency corresponds to an effective field of approximately 50 G. We then adiabatically demagnetized H_1 to a constant value, waited a variable time, and then increased H_1 to its original value. We then turned off H_1 sharply and, by observing the amplitude of the free-induction decay as a function of time in the demagnetized state, were able to measure $T_{1\rho}$.

A. Temperature Dependence of $T_{1\rho}$

Figure 4 shows a plot of the temperature dependence of $T_{1\rho}$ in the ultraslow-motion region for a single crystal[29] of TlCl along with a plot of T_2 for a pressed powder sample of TlCl. Figure 5 shows the temperature dependence of $(T_{1\rho})_{diff}$, the diffusion contribution to $T_{1\rho}$, which is obtained by subtracting the reciprocal of the low-temperature (or asymptotic) $T_{1\rho}$ from the measured relaxation rate. There are several significant features of the $T_{1\rho}$ data. First, for the temperature-dependent linear portion (on the semilog plot) of $(T_{1\rho})_{diff}$ we measure an activation energy of (0.733 ± 0.012) eV which agrees quite well with Friauf's results,[4] obtained using other methods.

A second feature of Fig. 4 is that the $T_{1\rho}$ minimum occurs considerably above the temperature corresponding to the onset of motional narrowing. This phenomenon is due largely to the existence of static quadrupole interactions which, according to Eq. (8), will cause the measured $T_{1\rho}$ to be shifted to values considerably higher than those resulting from dipolar interactions alone. As we shall see, further evidence for the existence of these static quadrupolar interactions is indicated by measurements of the dependence of $T_{1\rho}$ on H_1.

A third feature is the slight dip[30] at the shoulder separating the diffusion region from the asymptotic region. This dip appears to be real and has two possible explanations. The first possibility is that the dip is the diffusion minimum due to the quadrupole interaction between the chlorine atoms and vacancies (which should occur when the vacancy jump time τ_v is of the order of the mean quadrupole splitting). Since $\tau_v \ll \tau$, the quadrupole minimum would undoubtedly occur at a much lower temperature than the dipolar minimum. At all temperatures above this minimum the Cl-vacancy-quadrupole interaction should be motionally narrowed and should not contribute appreciably to the relaxation time.

A second possible explanation is that the dip is

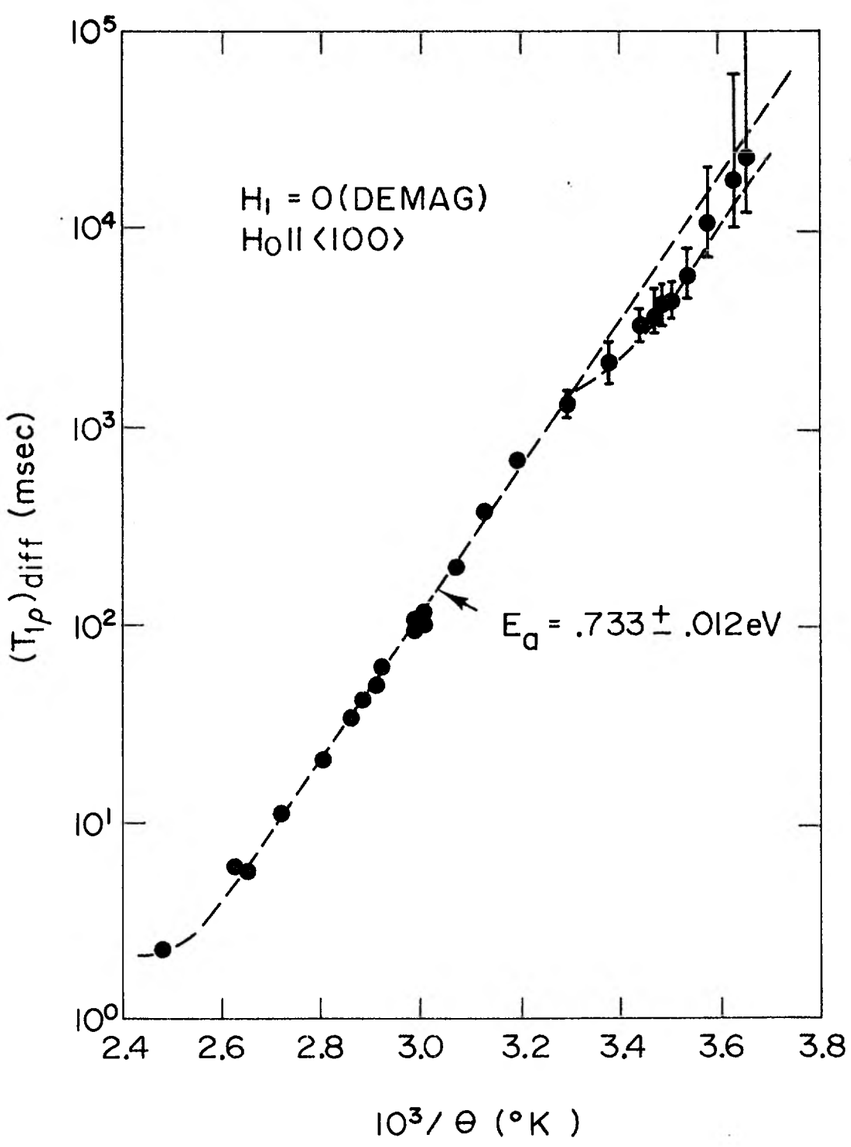

FIG. 5. $(T_{1\rho})_{diff}$ vs reciprocal temperature. These data are taken from the $T_{1\rho}$ data in Fig. 4, with the nondiffusion asymptotic contribution subtracted off, thereby giving the diffusion contribution to $T_{1\rho}$

really a shift in $T_{1\rho}$ caused by going from a high-temperature region for which $\tau_v < T_2$ to a lower-temperature region for which $\tau_v > T_2$. The main effect should be that, at the lower temperatures, $(T_{1\rho})_{\mathrm{diff}}$ will be reduced by a factor of order $(G-2)/G$ relative to its value at higher temperatures. In TlCl, for which $G=6$, this factor should be $\frac{2}{3}$. It is interesting to note that the reduction observed in Fig. 5 is of the order of $\frac{2}{3}$ within experimental error. If this interpretation is correct, τ_v at the temperature of the dip should be ~ 240 μsec (since it would equal the rigid lattice T_2). Using Eq. (8), we would obtain τ at this same temperature to be approximately $\frac{1}{4}$ sec. We then find that the vacancy concentration can be determined, since $N_v/N = \tau_v/\tau \cong 10^{-3}$. If the vacancies are produced thermally, we could then estimate the formation energy E_f of a vacancy, since

$$N_v/N = e^{-E_f/k\theta} . \tag{27}$$

Using Eq. (27) we obtain $E_f \cong 0.16$ eV. This explanation of the source of the dip is really only tentative. However, it fits the observations and suggests tantalizing possibilities for using NMR to measure the formation energy independent of the total activation energy.

In order to measure independently all the parameters in Eq. (8), it was necessary to determine τ. Since motional narrowing begins when $\tau \approx T_2$, we could use our T_2 data[31] from Fig. 4 to estimate τ. We somewhat arbitrarily assumed the onset of motional narrowing to occur at the intersection of the asymptotes to the high- and low-temperature T_2 data. Since a fraction $2/G$ of all jumps do not contribute to relaxation in the case $\tau_v \ll T_2$, τ in Eq. (8) should be replaced by an effective-jump-correlation time[32] equal to $\tau G/(G-2)$. Thus, for $\tau_v \ll T_2$, we replace Eq. (8) by

$$(T_{1\rho})_{\mathrm{diff}} = \frac{\tau(H_1^2 + H_D^2 + H_Q^2)}{2(1-p_D)H_D^2 + (1-p_Q)H_Q^2} \left(\frac{G}{G-2}\right) . \tag{28}$$

B. H_1 Dependence of $(T_{1\rho})_{\mathrm{diff}}$

Since $(T_{1\rho})_{\mathrm{diff}}$ in Eq. (28) has a linear dependence on H_1^2, a plot at a constant temperature in the ultraslow region of $(T_{1\rho})_{\mathrm{diff}}$ vs H_1^2 will intersect the H_1^2 axis at $-(H_D^2 + H_Q^2)$. We can thus measure the total local field. Figure 6 shows the results of one of four $(T_{1\rho})_{\mathrm{diff}}$ vs H_1^2 runs. The average of three runs with the sample oriented with H_0 parallel to the $\langle 100\rangle$ direction gives $H_D^2 + H_Q^2 = [(9.57 \pm 0.5)\ \mathrm{G}]^2$. Since the dipolar contribution H_D^2 was calculated in Sec. III A to be $(1.666 - 0.548 \sin^2 2\varphi)\ \mathrm{G}^2$, these experimental results indicate that the local field arises largely from static quadrupole interactions[33] due probably to strains, dislocations, and similar defects. In order to see whether the sources of quadrupole interaction were randomly oriented in our sample, we performed a fourth $(T_{1\rho})_{\mathrm{diff}}$ vs H_1^2 run with the sample oriented such that H_0 was parallel to the $\langle 110\rangle$ direction. We obtained the same local field, within experimental error, as in the $\langle 100\rangle$ runs.

In order to relate $(T_{1\rho})_{\mathrm{diff}}$ to $(1-p_D)$, we must first determine the quantity $(1-p_Q)H_Q^2$. Since the static quadrupolar interaction gives rise to a broadening which is independent of angle, we shall assume that $(1-p_Q)H_Q^2$ is also independent of angle. By using Eq. (28), we can relate the y intercept of Fig. 6 to $(1-p_Q)H_Q^2$, since all the other parameters have been either independently measured or calculated theoretically. We then obtain the value $(1-p_Q)H_Q^2 = (2.6 \pm 0.3)\ \mathrm{G}^2$.

The experimental technique used in measuring $T_{1\rho}$ vs H_1^2 is to perform the demagnetization of the z field in a large H_1 field followed by a partial demagnetization of H_1 to a reduced (though not necessarily zero) value.[34] After a suitable time interval H_1 is remagnetized to its original value and is then turned off sharply. By plotting for different H_1's, the amplitude of the subsequent free-induction decay as a function of time in the state of reduced

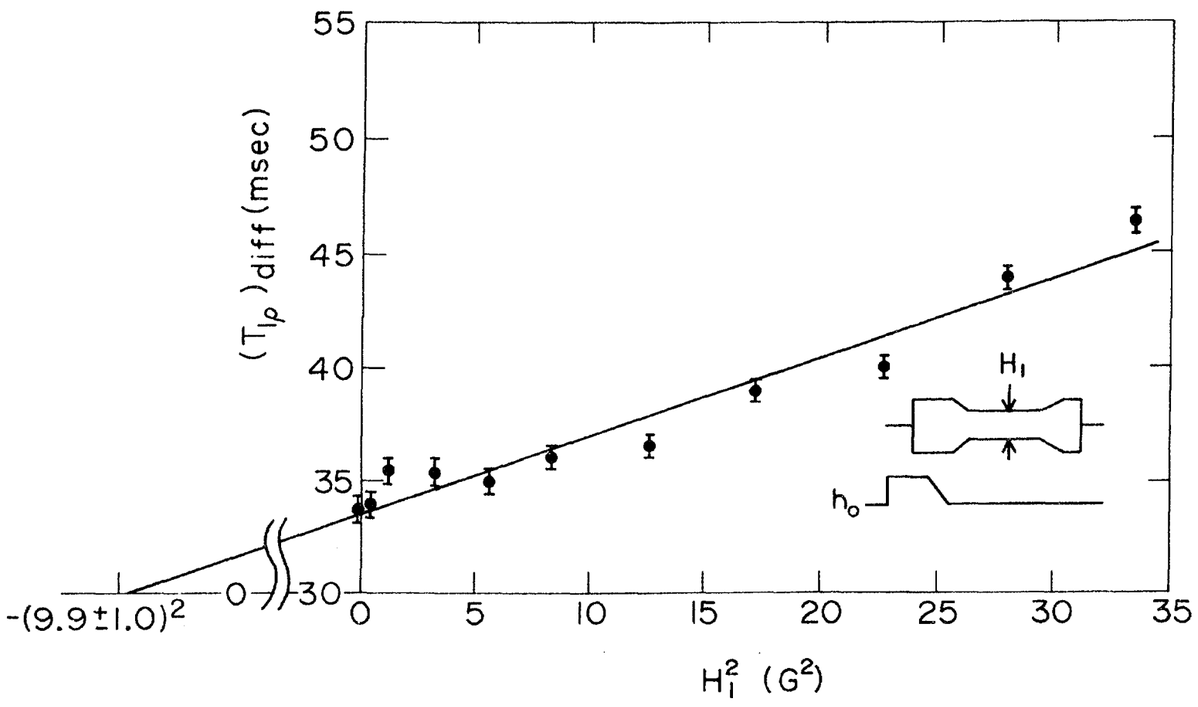

FIG. 6. $(T_{1\rho})_{\mathrm{diff}}$ vs H_1^2 data showing the intersection of the extrapolated best fit with the H_1^2 axis where $H_1^2 = -(H_D^2 + H_Q^2)$. H_0 is parallel to the $\langle 100\rangle$ direction and the temperature is (350.0 ± 0.2) °K. Also shown is the pulse sequence: H_1 refers to the rf field and h_0 is the off-resonant z field.

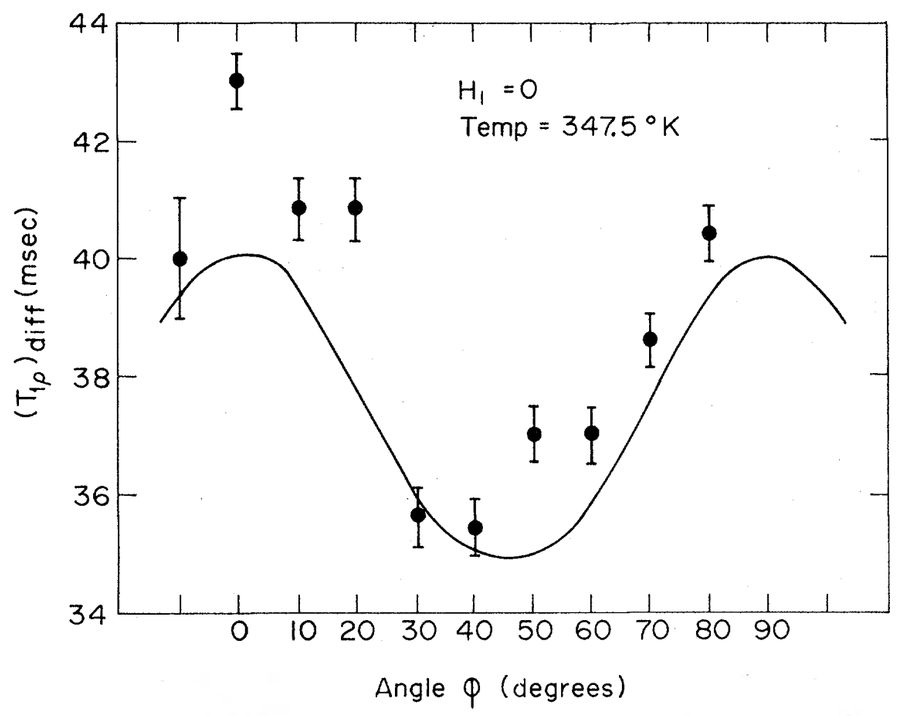

FIG. 7. $(T_{1\rho})_{diff}$ vs crystal orientation with $H_1 = 0$. The points represent experimental data and the solid line is a theoretical angular dependence determined from calculated and independently measured parameters.

H_1, we can measure $T_{1\rho}$ vs H_1.

A second method for determining the local field involves the direct measurement of M_x as a function of H_1 following an ADRF sequence. Slichter and Holton have shown that the equilibrium magnetization along H_1, after adiabatic demagnetization, is given by

$$M_x = M_0 H_1/(H_1^2 + H_L^2)^{1/2}\ , \qquad (29)$$

where H_L^2 is the square of the total local field (i.e., $H_D^2 + H_Q^2$). Because of the large sample volume over which H_1 was applied, we were limited to fields for which $H_1 \lesssim H_L$. Nevertheless, our data were consistent with a local field greater than 7 G which is in approximate agreement with the previous results.

C. Angular Dependence of $(T_{1\rho})_{diff}$

The primary contributor to the angular dependence of $T_{1\rho}$ should be the term $1 - p_D$ and this is the quantity which, according to the calculations of Ailion and Ho,[2] would be most sensitive to the details of the motion responsible for the relaxation. In the absence of quadrupolar effects, $(T_{1\rho})_{diff}$ in zero H_1 will be simply proportional to $(1 - p_D)^{-1}$ and so the angular dependence of $(T_{1\rho})_{diff}$ would then be identical to that of $(1 - p_D)^{-1}$.

The extra quadrupolar terms in the denominator of Eqs. (8) and (28) will have the principal effect of reducing the angular dependence of $(T_{1\rho})_{diff}$. Since we have independently measured all the parameters other than p_D and H_D^2 on the right side of Eq. (28), we can use their observed values along with the theoretical values of p_D and H_D^2 to obtain "theoretical" values for the angular dependence of $(T_{1\rho})_{diff}$ for different diffusion mechanisms. By comparing these curves with experiment we can distinguish between rival mechanisms if their angular dependences are sufficiently different. Figures 7 and 8 show comparisons of experimental and theoretical angular dependences for $H_1 = 0$ and $H_1 = 5.8$ G, respectively. For $H_1 = 0$, the theoretical angular dependence predicted by Eq. (28) for vacancy diffusion is 13.4% as compared to our observed results of $(15.0 \pm 2)\%$. For $H_1 = 5.8$ G, the agreement is even better, with a theoretical angular dependence of 14.3% and experimental of $(15.5 \pm 2)\%$. The very slight displacement of our experimental curves to the left is probably due to a slight misalignment of our crystal. The entire curves could be displaced vertically by a small error[32] in our determination of τ. It should be emphasized that our measurements of τ and H_Q^2 are independent of our measurements of $(T_{1\rho})_{diff}$. The value of $(1 - p_Q) \times H_Q^2$ is determined by our measurements of $(T_{1\rho})_{diff}$ at $\varphi = 0$ and $H_1 = 0$. Our measurements of $(T_{1\rho})_{diff}$ at $\varphi = 45°$ then provide an independent check on our theoretical angular dependence.

It is instructive to compare our observed angular dependence with the results obtained from an alternative mechanism. If we consider the admittedly unlikely possibility of Cl interstitialcy diffusion in which the Cl interstitial atom is centered between two Tl sites, we can then calculate the angular dependence of $(1 - p_D)$ for interstitialcy jumps (see Fig. 1). The details of this calculation are worked out in Ref. 17. For the $H_1 = 0$ case, these calculations predict a 9.8% angular dependence, whereas, for the $H_1 = 5.8$ G, they predict a 9.0% dependence. Since both of these results deviate considerably from the experimental values of $(15.0 \pm 2)\%$ and $(15.5 \pm 2)\%$ for the two H_1's, we can exclude Cl interstitialcy diffusion as a dominant mechanism in TlCl.[35]

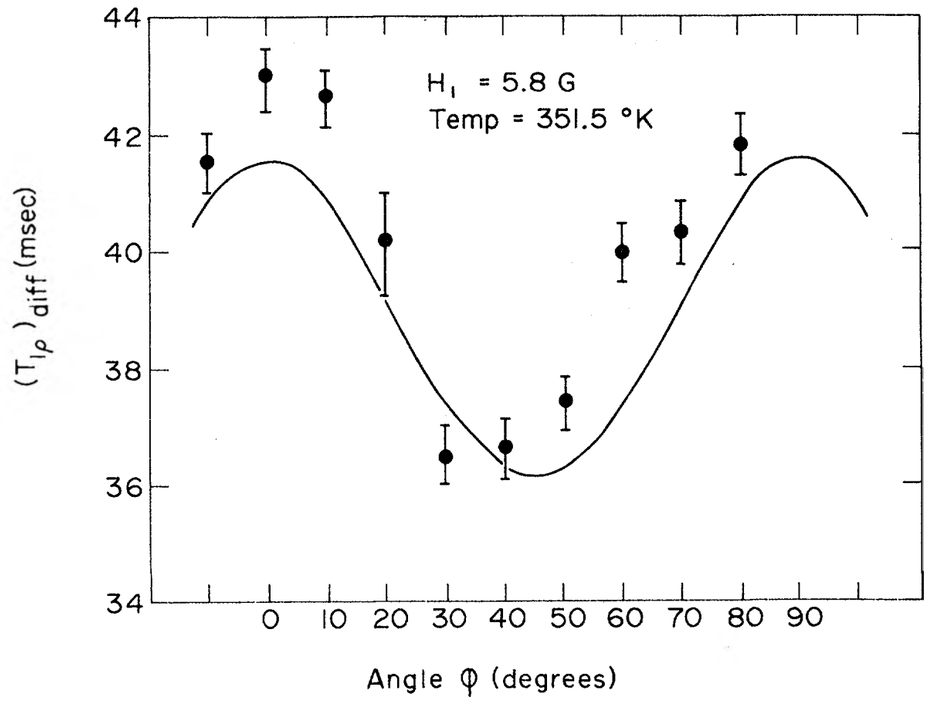

FIG. 8. $(T_{1\rho})_{diff}$ vs crystal orientation as in Fig. 7 but with $H_1 = 5.8$ G.

VI. CONCLUSIONS

In this paper we have described the experimental verification of the prediction of Ailion and Ho that the rotating-frame spin-lattice relaxation time $T_{1\rho}$ would have an angular dependence in the ultraslow-motion region which is sensitive to diffusion mechanism. In particular we performed our experiments in TlCl, a substance in which the diffusion mechanism has been independently determined by Friauf to be Cl vacancy diffusion. We obtained excellent agreement between our experimental results and our theory which assumes diffusion to result from the motion of Cl vacancies, whereas our data disagreed with the results of calculations based on an interstitialcy model for diffusion. Similar experiments and comparisions may be used to determine the dominant diffusion in other substances.

ACKNOWLEDGMENTS

The authors wish to thank Robert Morse for his assistance in writing the computer programs used in calculating the lattice sums. They are grateful to Dr. Franz Rosenberger of the University of Utah Crystal Growth Laboratory for growing the TlCl crystal. Discussions with D. Wolf, Dr. D. Alderman, Professor T. J. Rowland, Professor P. R. Moran, Professor I. J. Lowe, Professor J. S. Waugh, and especially Professor C. P. Slichter have been particularly valuable.

One of the authors (G. L. S.) is grateful to the federal government for providing a 3-year NDEA IV fellowship.

APPENDIX: CALCULATION OF $1-p_D$ FOR THE CASE $\tau_v \gg T_2$

This calculation is similar to the one originally performed by SA in lithium.[5] It can be handled considerably more easily than the $\tau_v \ll T_2$ case since now the vacancy waits until all spins near it are in equilibrium before jumping again. Even return jumps are considered as independent contributions to the relaxation; therefore, there is no spin trail to consider. In going from a spin sum to a lattice sum, the site of the neighboring vacancy must be excluded explicitly from the sum in the II and II' contributions to $\langle \Delta E \rangle_D$. We then have[17] for $\tau_v \gg T_2$ that

$$(1-p_D)=\frac{\hbar^2 f_I \gamma_I{}^2 I(I+1)}{4a^6 H_D{}^2}\left[\left(1+\frac{2f_{I'}\gamma_{I'}{}^2}{3f_I\gamma_I{}^2}\right)\left(\sum_i C_{ir}{}'^2 - C_{qr}{}^2 - \sum_i C_{ir}C_{iq}\right)+\frac{2S(S+1)}{3I(I+1)}\left(\frac{f_S\gamma_S{}^2}{f_I\gamma_I{}^2}+\frac{f_{S'}\gamma_{S'}{}^2}{f_I\gamma_I{}^2}\right)\right.$$
$$\left.\times\left(\sum_s C_{sr}{}'^2 - \sum_s C_{sr}C_{sq}\right)\right]=\frac{0.0240+0.1948\sin^2 2\varphi}{1.666-0.548\sin^2 2\varphi}\,. \quad \text{(A1)}$$

† This research has been supported by the National Science Foundation under Grant No. GP-17412 and in part by the Research Corporation.

*This paper is based in part on the Ph. D. thesis presented by G. L. Samuelson, at the University of Utah, Salt Lake City (unpublished).

[1] A preliminary version of this work is to appear in an article by the above authors, in Proceedings of the XVIth Colloquium AMPERE, Bucharest, 1970 (unpublished).

[2] D. C. Ailion and P. Ho, Phys. Rev. 167, 662 (1968).

[3] A review of the ultraslow-motion techniques can be found in the article by D. C. Ailion, Advan. Magnetic Resonance 5, 177 (1971).

[4] R. J. Friauf, J. Phys. Chem. Solids 18, 203 (1961); also private communication.

[5] C. P. Slichter and D. C. Ailion, Phys. Rev. 135, A1099 (1964).

[6] N. Bloembergen, E. M. Purcell, and R. V. Pound, Phys. Rev. 73, 679 (1948).

[7] H. C. Torrey, Phys. Rev. 92, 962 (1953); 96, 690 (1954).

[8] D. C. Look and I. J. Lowe, J. Chem. Phys. 44, 2995 (1965); 44, 3437 (1965).

[9] D. C. Ailion and C. P. Slichter, Phys. Rev. 137, A235 (1965).

[10] L. C. Hebel and C. P. Slichter, Phys. Rev. 113, 1504 (1959).

[11] A. Abragam, *The Principles of Nuclear Magnetism* (Clarendon, Oxford, England, 1961), p. 65.

[12] A. G. Redfield, Phys. Rev. 98, 1787 (1955).

[13] C. P. Slichter and W. C. Holton, Phys. Rev. 122, 1701 (1961).

[14] John Waugh and co-workers have recently shown that the existence of a spin temperature does not require the vanishing of *all* the off-diagonal density-matrix elements but rather only the vanishing of operators like ρM_x. Moreover, they showed that the density operator is not correctly described by Eq. (1); Eq. (1) would be correct, however, for a density matrix *averaged* over a coarse region of phase space. In order to observe the nonrandomness of the offdiagonal elements they applied a pulse sequence which effectively reverses time (by changing the sign of the Hamiltonian). [See W. K. Rhim, A. Pines, and J. S. Waugh, Phys. Rev. Letters 25, 220 (1970); Phys. Rev. 3, 684 (1971).] Since nowhere in the ultraslow-motion experiments is the Hamiltonian reversed, a treatment based on Eq. (1) will yield the correct answer.

[15] T. J. Rowland and F. Y. Fradin, Phys. Rev. 182, 760 (1969).

[16] J. Wagner, Ph. D. thesis (University of Wisconsin 1970 (unpublished).

[17] G. L. Samuelson, Ph. D. thesis (University of Utah, 1971 (unpublished).

[18] The detailed steps in this calculation are given in Ref. 17. We will just outline the essential features here.

[19] Effects of encounters have been considered in detail

by Redfield and Eisenstadt [Phys. Rev. 132, 635 (1963)].

[20]Our treatment for this case differs from that used in Ref. 2, since the authors of that article calculated the energy change resulting from one jump. Since the spin system has not achieved a temperature prior to the next vacancy jump, they had to estimate an equivalent temperature in order to calculate the final energy. Our treatment avoids this difficulty and also includes the contribution to the energy change resulting from the vacancy's approach from an infinite distance to a site neighboring our atom of interest as well as the contribution resulting from the vacancy's departure to infinity after the jump.

[21]The apparatus is described in considerably more detail in Ref. 17.

[22]S. R. Hartmann and E. L. Hahn, Phys. Rev. 128, 2042 (1962).

[23]G. L. Samuelson and D. C. Ailion, Rev. Sci. Instr. 41, 743 (1970).

[24]R. J. Blume, Rev. Sci. Instr. 32, 1016 (1961).

[25]F. M. Lurie, Ph. D. thesis (University of Illinois, 1963 (unpublished).

[26]G. L. Samuelson and D. C. Ailion, Rev. Sci. Instr. 41, 1601 (1970).

[27]The company manufacturing these multichannel analyzers is now referred to as Nicolet Instrument Corp. and is no longer a subsidiary of Fabri-Tek, Inc.

[28]It is critical that the demagnetization be adiabatic. Because of the small γ of Cl^{35}, the adiabatic condition puts stringent requirements on the minimum demagnetization time. If the demagnetization is too rapid for the magnetization to follow, the magnetization will be left in the xz plane pointing in a direction other than H_1. A "two-component" relaxation will then be observed (see Ref. 17). The first component results from the transverse decay of the magnetization component perpendicular to H_1 in a time of the order of T_2, whereas the second component will be the normal $T_{1\rho}$ decay of the magnetization component parallel to H_1.

[29]The crystal was grown in the University of Utah Crystal Growth Laboratory from high-purity powdered TlCl obtained from Alfa Inorganics, Inc. Even though the starting material was stated to have a purity with respect to heavy-metal impurities of 10 ppm, we further purified it by means of a vacuum distillation prior to crystal growth.

[30]Similar effects have been observed in doped LiF samples by Wagner and Moran [J. Wagner, Ph. D. thesis (University of Wisconsin, 1970) (unpublished)].

[31]It would have been preferable to perform the T_2 experiments on our single crystal rather than on a powder sample. However, these measurements were performed prior to the $T_{1\rho}$ measurements and our apparatus was subsequently modified. Because of the over-all consistency of our results, it appears that small errors in the determination of τ are not significant in our $(1-p_D)^{-1}$ determinations.

[32]We have neglected the fact that the mean time between atomic jumps is not precisely the mean time between encounters since a vacancy will have a relatively high probability of causing a nearby atom to undergo additional jumps before the vacancy departs (see Ref. 19). When $\tau_v \ll T_2$, such extra jumps will not contribute to the relaxation and thus we are really observing the mean time between encounters. These effects are only partially included in our factor $G/(G-2)$. D. Wolf (private communication) has calculated that a determination of τ which neglects the effects of encounters could be in error by as much as 30%.

[33]We can not *absolutely* conclude that the extra broadening is due to quadrupolar effects. Another possible source of broadening could arise from the indirect couplings between the Cl and Tl nuclei. However, because of the large antishielding factor of Cl^{35} along with its relatively smaller atomic number, we felt that the broadening is more likely to be due to quadrupolar effects. Moreover, the free-induction decay appears to be Gaussian which is consistent with the idea that it is due to random defects.

[34]It is necessary to perform the z demagnetization in a large H_1 in order to ensure that it will be adiabatic, since the smallness of γ for Cl^{35} makes the adiabatic condition quite stringent for small H_1's.

[35]It is interesting to note that $G=4$ for interstitialcy diffusion in TlCl since there are four nearest-neighbor sites to which the Cl interstitial may jump. Thus, for the case $\tau_d \ll T_2$, the factor $(G-2)/G$ will be different for the two mechanisms. Accordingly, the absolute value of $(T_{1\rho})_{\text{diff}}$ could also be used to distinguish between rival mechanisms *provided* τ can be determined with sufficient accuracy.